Decomposition of group-velocity-locked-vector-dissipative-soliton and the recombination

XUAN WANG,[1] LEI LI,[1] YING GENG,[1] HANXIAO WANG,[1] LEI SU,[2] LUMING ZHAO[1, 3, *]

1. Jiangsu Key Laboratory of Advanced Laser Materials and Devices, Jiangsu Collaborative Innovation Center of Advanced Laser Technology and Emerging Industry, School of Physics and Electronic Engineering, Jiangsu Normal University, Xuzhou, Jiangsu 221116 China
2. School of Engineering and Materials Science, Queen Mary University of London, London, UK
3. Key Laboratory of Optoelectronic Devices and Systems of Ministry of Education and Guangdong Province, Shenzhen University, 518060, China
** Corresponding author: zhaoluming@jsnu.edu.cn*

By using a polarization manipulation and projection system, we numerically decomposed the group-velocity-locked-vector-dissipative-solitons (GVLVDSs) from a normal dispersion fiber laser and studied the combination of the projections of the phase-modulated components of the GVLVDS through a polarization beam splitter. Pulses with structure similar to a high-order vector soliton could be obtained, which could be considered as a pseudo-high-order GVLVDS. It is found that, although GVLVDSs are intrinsically different from group-velocity-locked-vector-solitons (GVLVSs) generated in fiber lasers operated in the anomalous dispersion regime, similar characteristics for the generation of pseudo-high-order GVLVDS are obtained. However, pulse chirp plays a significant role on the generation of pseudo-high-order GVLVDS.

1. INTRODUCTION

Dissipative solitons (DSs) can be generated in fiber lasers with normal dispersion, due to the combined effects among fiber nonlinearity, cavity dispersion, gain and loss, spectral filtering, etc. [1-5] Different from the conventional solitons obtained in fiber lasers operated in the anomalous dispersion regime, DSs are generally chirped pulses. Various mode-locking techniques, such as the nonlinear polarization rotation technique [1, 6] and the using of saturable absorber [7], can achieve DS generation in fiber laser.

Due to the existence of intrinsic birefringence from fibers and the randomly applied external pressure, vector solitons (VSs) can be generated in fiber lasers provided that there is no polarization-dependent component in the cavity [8]. VSs refer to a pulse with multiple components, and all the components propagate as a unit in media. When the fiber laser is operated in the normal dispersion regime, DSs along orthogonal polarization directions can bind together and propagate as a unit, consequently a vector dissipative soliton (VDS) is generated [9]. Either coherently coupled VDSs or incoherently coupled VDSs could be generated in fiber lasers [10]. The trapping between different components of a VS can be resulted from group-velocity locking [11] or phase locking [8]. Specifically, for group-velocity-locked VSs (GVLVSs), a wavelength shift between the two orthogonal components of a VS could exist, which results in the propagation speed compensation to the group velocity difference due to birefringence [11, 12]. Similar situation happens for the group-velocity-locked VDSs (GVLVDSs) although GVLVDSs have typical steep spectral edges and large chirp while GVLVSs have Kelly sidebands and almost zero chirp. Apart from the fundamental VSs, high-order VSs have been demonstrated in a passively mode-locked fiber laser [13], where the two polarization components of the VS are phase-locked. There is a two-humped temporal profile along one polarization, while a single-humped pulse is observed along the orthogonal polarization. The observation of high-order VSs significantly expands our understanding of soliton dynamics in fiber lasers.

To obtain a high-order VS, nearly zero cavity birefringence is required and critical operation conditions should be satisfied [13]. Our group has proposed a simple method to obtain pulse structure similar to a high-order VS [14]. By recombining the projections of a phase-modulated fundamental GVLVS, pulse structure similar to a high-order VS that has a double-humped pulse profile along one polarization while a single-humped pulse profile along the orthogonal polarization direction, could be achieved with appropriate setting of the time separation between the two orthogonally polarized components of the fundamental VS. We further experimentally demonstrated our proposal [15]. When a fundamental GVLVS with appropriate component separation went through a polarization controller (PC), phase retard was imposed on the two polarization components of the GVLVS, which would simultaneously change the directions of two orthogonally polarized components. After projecting respectively on the two polarization axes of the following polarization beam splitter (PBS), the combination of projections from the two phase-modulated polarization components of the GVLVS might result in a double-humped pulse profile along one polarization axis while a single-humped pulse profile along the other polarization axis of the PBS. The combined pulses along the two polarization axes of the PBS did not lock together. However, under appropriate phase modulation resulted from the PC, the optical spectra of the combined projections along the horizontal/vertical axis could be same to those of a high-order GVLVS, as well as the intensity profile. The central

wavelength of the two constructed pulses along the two axes of the PBS could also be same, which means they will have same group velocity if using them as the two polarization components of a VS and let them propagating in a fiber. Therefore, we call it "pseudo-high-order GVLVS."

Our simple scheme to construct a pseudo-high-order GVLVS makes the realization of a high order GVLVS with controllable parameters possible, which is helpful both in the fundamental research for further understanding soliton dynamics and in the potential applications such as telecommunications. VSs are a natural seed source for ternary system. As GVLVDSs are essentially different from GVLVSs, for example, GVLVDSs are generally chirped while GVLVSs are almost transform-limited, in this paper, numerical simulations were carried out to test similar procedure to construct a pseudo-high-order GVLVDS based on a fundamental GVLVDS. It is found that the structure of a "pseudo-high-order GVLVDS" can be generated from a fundamental GVLVDS even when the component separation of the GVLVDS is far smaller than the component duration. Artificially constructed GVLVDSs with different pulse parameters are tested. It is found that not all GVLVDSs could result in the structure of a "pseudo-high-order GVLVDS". Parameters of the GVLVDSs, especially the chirp of the GVLVDS, significantly affect the final structure of the "pseudo-high-order GVLVDS".

2. THEORETICAL MODEL

The phase modulation and polarization resolved system is same as that in Ref. [14]. As shown in Fig. 1, a PC is used to impose phase modulation on the tested GVLVDS, then a PBS is used to separate the projections of the two phase-modulated components of the GVLVDS. The two output polarization-maintaining branches of the PBS is set to be strictly identical. The basic parameters of pulse duration and chirp of the tested GVLVDSs are from a fundamental GVLVDS generated from a home-made fiber laser [16]. The fiber laser is dispersion-managed but operated in the normal dispersion regime. A transmission-type semiconductor saturable absorber is used to

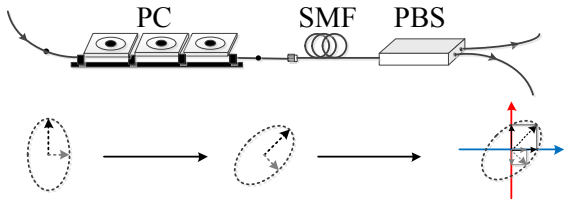

Fig. 1 The phase modulation and polarization resolved system. PC: polarization controller; SMF: single-mode-fiber; PBS: polarization beam splitter

achieve the mode locking. By tuning the in-line PC with pump power, fundamental GVLVDSs are expected. Generally the GVLVDS has a pulse duration of ~3.7 ps and a 3-dB bandwidth of ~7.9 nm. Therefore, the chirp parameter is about 3.6 if a chirped Gaussian pulse is assumed [17].

The two polarizations of the GVLVDS after traversing the PC can be expressed as the followings:

$$U_1(T) = \sqrt{I_1}e^{-\frac{1.665^2(1+iC_1)}{2}\left(\frac{T-\frac{\Delta T}{2}}{T_1}\right)^{2m}} e^{i\left(\frac{2\pi cT}{\lambda_1}\right)} \quad (1)$$

$$U_2(T) = \sqrt{I_2}e^{-\frac{1.665^2(1+iC_2)}{2}\left(\frac{T+\frac{\Delta T}{2}}{T_2}\right)^{2m}} e^{i\left(\frac{2\pi cT}{\lambda_2}+\Delta\varphi\right)} \quad (2)$$

where we assume the polarization components of the GVLVDS both have a Gaussian profile. I_1 and I_2 are intensity of the two polarization components of the GVLVDS. T_1 and T_2 are the corresponding pulse duration of the two polarization components, ΔT is the time delay between the two polarization components. m is the order of the pulse, here m=1. λ_1 and λ_2 are the central wavelength of the optical pulses along the two orthogonal polarizations. $\Delta\varphi$ is the phase difference between the two components, which is resulted from the initial phase difference plus phase difference caused by the PC. C_1 and C_2 are the chirp parameters. The constructed pulse can be expressed by equation (3) and (4). θ is the projected angle between the horizontal axis of the PBS and the U_1. The output pulses along the horizontal axis and the vertical axis are the superposed results of projections.

$$U_{Horizontal} = U_1 cos\theta + U_2 cos(\theta + 1.5\pi) \quad (3)$$

$$U_{Vertical} = U_1 sin\theta + U_2 sin(\theta + 1.5\pi) \quad (4)$$

3. SIMULATION RESULTS AND DISCUSSIONS

In the simulations, the following parameters are used if not specifically set: T_1=T_2=4 ps; C1=C2=3.6. Depending on the cavity birefringence and detailed operation conditions, the central wavelength of the two orthogonally polarized components of the GVLVDS could be changed together with the amplitude [16].

We first studied the case when the cavity birefringence is small, which corresponds to that the central wavelength separation of the two orthogonal polarization components of the GVLVDS is close to zero. The intensity of the two components are set as I_1=I_2=10 W; λ_1=λ_2=1565 nm. 1) Similar to the case of GVLVS [14], when θ=0, no matter what the value of $\Delta\varphi$ and ΔT is, the pulse intensity profiles along the horizontal and vertical axis are both single-humped and the spectral components along the horizontal and vertical axis have the same central wavelength, as shown in Fig. 2, where the spectrum are overlapped due to the same pulse intensity. 2) When θ≠0, spectral dip may appear on the spectrum of the two axes and the position of the spectral dip depends on Δφ and ΔT, as shown in Fig. 3. However, the temporal dip may not be down to zero. One special case is when θ≠0 but ΔT=0, no matter what the value of Δφ is, the pulse intensity profiles along the horizontal and vertical axis are both single-humped. 3) Depending on the pulse intensity of the two components of the GVLVDS, with appropriate selection of θ, here θ=45°, strong dip could be formed in the middle of spectrum with appropriate Δφ, here Δφ=0°, as shown in Fig. 4. There are a two-humped pulse along the vertical axis and a single-humped pulse along the horizontal axis. The two-humped/single-humped pulse is the combination of two projections from the phase-modulated components of the GVLVDS

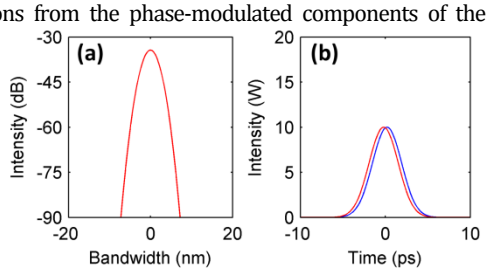

Fig. 2 (a) Optical spectra, and (b) pulse profiles along horizontal axis (blue) and vertical axis (red) when θ=0°, ΔT=0.4 ps.

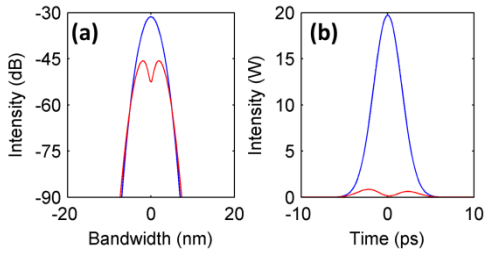

Fig. 3 (a) Optical spectra, and (b) pulse profiles along horizontal axis (blue) and vertical axis (red) when θ=40°, ΔT=0.4 ps, Δφ=0.

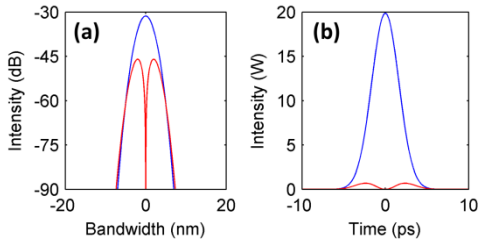

Fig. 4 (a) Optical spectra, and (b) pulse profiles along horizontal axis (blue) and vertical axis (red) when θ=45°, ΔT=0.4 ps, Δφ=0.

while the phase difference between corresponding projections is 180°/0°. The central wavelength of the two re-constructed pulses are same. Therefore, the aggregation consisting of the two re-constructed pulses can be considered as a "1+2" pseudo-high-order GVLVDS.

The impact of the time delay between the two polarization components is explored. It is found that, when the time delay is zero, no pseudo-high-order GVLVDS could be generated. Once the time delay exists, pseudo-high-order GVLVDS could be generated. Figure 5 shows the pulse features when all the parameters are same as those in Fig. 4 and the time delay varies from 0 to 2 ps. Figure 5(a) and Fig. 5(b) show the profile evolution along the vertical axis and the horizontal axis, respectively. The pulse duration of the horizontal peak and the vertical peak both decrease with the increase of the time delay as shown in Fig. 5(c). The intensity of the two-humped pulse increases while the hump separation of the two-humped pulse decreases with the time delay increasing as shown in Fig. 5(d). When 0≤ΔT≤2 ps, typical structure similar to Fig. 4 can be obtained. The temporal dip along the vertical axis is always down to zero. More structure that is complex would appear along both axes when the time delay between the two polarization components further increases, which is caused by the chirp. Figure 6 and Fig. 7, respectively, shows for example the pulses along both axes when ΔT=4 ps with chirp and without chirp. The existence of chirp broadens the spectra and complicate the temporal profiles along both axes. When ΔT>12 ps, pseudo-high-order GVLVDS with two humps along both axes with clear pulse profiles can be obtained, in another word, a "2+2" pseudo-high-order GVLVDS is generated.

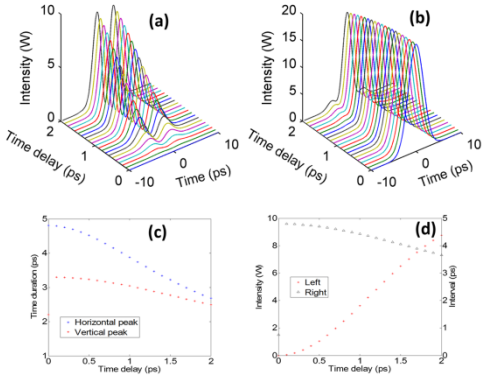

Fig. 5 Pulse evolution along the vertical axis (a), the horizontal axis (b) when time delay varies; (c) time duration of the horizontal peak and the vertical peak versus time delay; (d) the intensity and the hump separation of the two-humped pulse versus time delay.

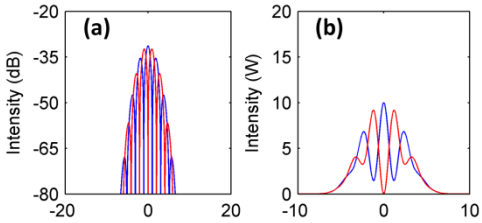

Fig. 6 (a) Optical spectra, and (b) pulse profiles along horizontal axis (blue) and vertical axis (red) when θ=45°, ΔT=4 ps, Δφ=0, and C_1=C_2=3.6.

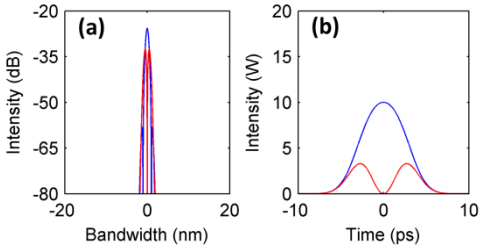

Fig. 7 (a) Optical spectra, and (b) pulse profiles along horizontal axis (blue) and vertical axis (red) when θ=45°, ΔT=4 ps, Δφ=0, and C_1=C_2=0

We then studied the case when the cavity birefringence is moderate, which means the central wavelength separation of the two orthogonal polarization components of the GVLVDS is obvious.

Here we used λ_1=1565 nm, λ_2=1566 nm. 1) When θ=0, no matter what the value of Δφ and ΔT is, the pulse intensity profiles along the horizontal and vertical axis are both single-humped as shown in Fig. 8. 2) When θ≠0, spectral dip may appear on the spectrum of the two axes and the position of the spectral dip depends on Δφ and ΔT. Specifically, as shown in Fig. 9, pseudo-high-order GVLVDS ("1+2") can be obtained even when $\Delta T = 0$, which is different from the case when the central wavelength separation is zero. Figure 10 shows a general example when $\Delta T = 0.4$ ps, θ=45°, Δφ=0.

The impact of ΔT on pulse characteristics is also examined. Figure 11 shows pulse features when ΔT varies while θ=45°, Δφ=0. The pulse duration of the horizontal peak and the vertical peak both first increases then decreases with the increase of the time delay as shown in Fig. 11(c). The intensity of the two-humped pulse decreases first then increases while the hump separation of the two-humped pulse increases first then decreases with the time delay increasing as shown in Fig. 11(d). When 0≤ΔT≤3 ps, typical structure similar to Fig. 4 can be obtained. The temporal dip along the vertical axis is always down to zero. Comparing with the case of λ_1=λ_2, apart from that when the time

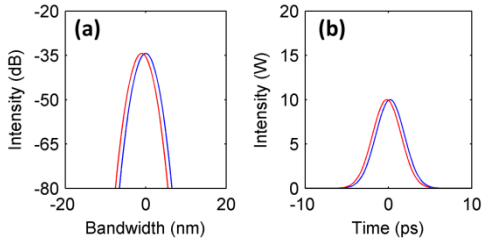

Fig. 8 (a) Optical spectra, and (b) pulse profiles along horizontal axis (blue) and vertical axis (red) when θ=0°, ΔT=0.4 ps, while λ_1=1565 nm, λ_2=1566nm.

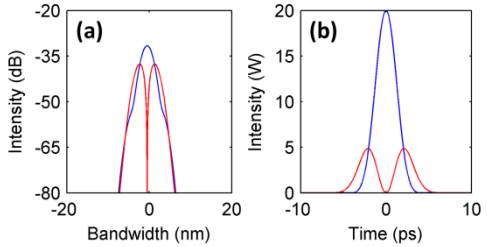

Fig. 9 (a) Optical spectra, and (b) pulse profiles along horizontal axis (blue) and vertical axis (red) when ΔT=0, θ=45°, Δφ=0, while λ1=1565 nm, λ2=1566nm.

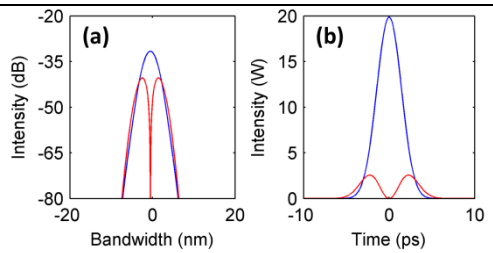

Fig. 10 (a) Optical spectra, and (b) pulse profiles along horizontal axis (blue) and vertical axis (red) when θ=45°, ΔT=0.4 ps, Δφ=0, while λ_1=1565 nm, λ_2=1566nm.

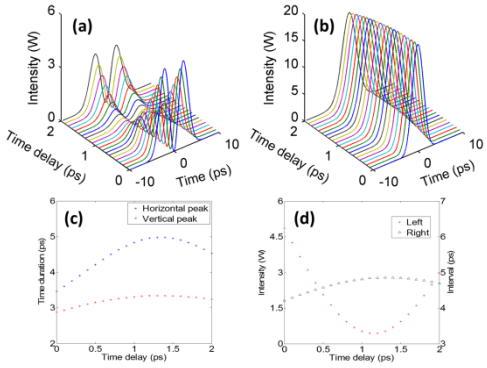

Fig. 11 Pulse evolution along the vertical axis (a), the horizontal axis (b) when time delay varies; (c) time duration of the horizontal peak and the vertical peak versus time delay; (d) the intensity and the hump separation of the two-humped pulse versus time delay when λ_1=1565 nm, λ_2=1566 nm.

delay is zero pseudo-high-order GVLVDS could be generated, the range for clear pseudo-high-order GVLVDS generation is bigger, which could be up to around 3 ps. Similar to the case of λ_1=λ_2, more complicated structure also appeared along both axes when the time delay between the two polarization components further increases, which is caused by the chirp. "2+2" type pseudo-high-order GVLVDS can be generated when ΔT>12 ps.

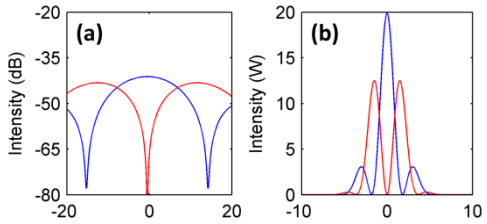

Fig. 12. (a) Optical spectra, and (b) pulse profiles along horizontal axis (blue) and vertical axis (red) when θ=45 °, ΔT=0.4 ps, Δφ=0, and C_1=C_2=36, while λ_1=1565 nm, λ_2=1566nm.

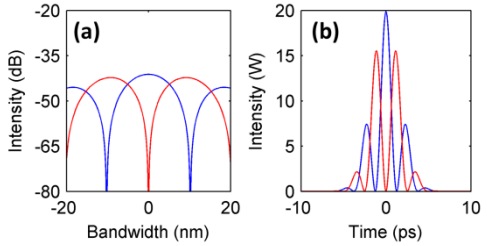

Fig. 13 (a) Optical spectra, and (b) pulse profiles along horizontal axis (blue) and vertical axis (red) when θ=45 °, ΔT=0.4 ps, Δφ=0, and C_1=C_2=36, while λ_1= λ_2=1565nm.

The influence of chirp on pulse features are considered. The chirp parameter is determined by the pulse duration and pulse bandwidth. Numerically we calculated the case when the chirp parameters were ten times of the experimental data. Figure 12 shows the case of different central wavelength, while Fig. 13 show the case of same central wavelength. It is found that bigger chirp results in broader bandwidth and larger spectral modulation period. Consequently narrower hump separation along either axis is obtained. The existence of different central wavelength plays a similar role as larger chirp.

4. CONCLUSIONS

Pseudo-high-order GVLVDSs are numerically demonstrated by combination of two orthogonally polarized pulses constructed from the projections of a phase-modulated GVLVDS. By propagating a fundamental GVLVDS through a PC following by a PBS, "1+2" or "2+2" type pseudo-high-order GVLVDSs can be generated depending on the detailed parameters of the fundamental GVLVDS. The impact of the angle between the horizontal polarized component of the GVLVDS and the horizontal axis of the PBS, the phase difference between the two phase-modulated components, the time delay between the two polarization components, and the chirp are discussed in details. Comparing with GVLVS without chirp, the existence of chirp in GVLVDS results in broader bandwidth and narrower hump separation in the generated pseudo-high-order GVLVDS.

Funding. Key Research Program of Natural Science of Jiangsu Higher Education Institutions (17KJA416004); National Natural Science Foundation of China (NSFC) (11674133, 11711530208, 61575089, and 61405079); Royal Society [IE161214]; Jiangsu Province Science Foundation (BK20140231); the Jiangsu Normal University, Xuzhou, China, through the Graduate Students in Research and Innovation Program (XYLX16-1323).

Acknowledgment. We thank the Priority Academic Program Development of Jiangsu higher education institutions (PAPD), and the Key Laboratory of Optoelectronic Devices and Systems of Ministry of Education and Guangdong Province.

References

1. L. M. Zhao, D. Y. Tang, and J. Wu, "Gain-guided soliton in a positive group-dispersion fiber laser," Opt. Lett. 31, 1788-1790 (2006).
2. N. Akhmediev, and A. Ankiewicz, "Dissipative Solitons: From Optics to Biology and Medicine," Lecture Notes in Physics 751 (2008).
3. W. Chang, J. M. Soto-Crespo, A. Ankiewicz, and N. Akhmediev, "Dissipative soliton resonances in the anomalous dispersion regime," Phys. Rev. A 79, 1039-1044 (2009).
4. P. Grelu, S. Chouli, J. M. Soto-Crespo, and W. Chang, "Dissipative solitons for mode-locked fiber lasers," Nat. Photonics 6, 84-92 (2012).
5. G. D. Shao, Y. F. Song, L. M. Zhao, D. Y. Shen, and D. Y. Tang, "Vector Gain-Guided Dissipative Solitons in a Net Normal Dispersive Fiber Laser," IEEE Photonic. Tech. L. 28, 975-978 (2016).
6. W. H. Renninger, A. Chong, and F. W. Wise, "Dissipative solitons in normal-dispersion fiber lasers," Phys. Rev. A 77, 681-700 (2008).
7. H. Zhang, D. Tang, R. J. Knize, L. Zhao, Q. Bao, and K. P. Loh, "Graphene mode locked, wavelength-tunable, dissipative soliton fiber laser," Appl. Phys. Lett. 96, 111112 (2010).
8. S. T. Cundiff, B. C. Collings, and W. H. Knox, "Polarization locking in an isotropic, modelocked soliton Er/Yb fiber laser," Opt. Express 1, 12-20 (1997).
9. L. M. Zhao, D. Y. Tang, X. Wu, and H. Zhang, "Dissipative soliton trapping in normal dispersion-fiber lasers," Opt. Lett. 35, 1902-1904 (2010).
10. L. M. Zhao, D. Y. Tang, H. Zhang, and X. Wu, "Bound States of Vector Dissipative Solitons," IEEE Photonics Journal 7 (2015).
11. L. M. Zhao, D. Y. Tang, H. Zhang, X. Wu, and N. Xiang, "Soliton trapping in fiber lasers," Opt. Express 16, 9528-9533 (2008).
12. Y. Wang, S. Wang, J. Luo, Y. Ge, L. Li, D. Tang, D. Shen, S. Zhang, F. W. Wise, and L. Zhao, "Vector Soliton Generation in a Tm Fiber Laser," IEEE Photonic. Tech. L. 26, 769-772 (2014).
13. D. Y. Tang, H. Zhang, L. M. Zhao and X. Wu, “Observation of high-order polarization-locked vector solitons in a fiber laser,” Phys. Rev. Lett. 101, 153904 (2008).
14. X. X. Jin, Z. C. Wu, Q. Zhang, L. Li, D. Y. Tang, D. Y. Shen, S. N. Fu, D. M. Liu, and L. M. Zhao, "Generation of High-Order Group-Velocity-Locked Vector Solitons," IEEE Photonics Journal 7 (2015).
15. X. X. Jin, Z. C. Wu, L. Li, Q. Zhang, D. Y. Tang, D. Y. Shen, S. N. Fu, D. M. Liu, and L. M. Zhao, "Manipulation of Group-Velocity-Locked Vector Solitons From Fiber Lasers," IEEE Photonics Journal 8 (2016).
16. Y. Y. Luo, L. Li, D. M. Liu, Q. Z. Sun, Z. C. Wu, Z. L. Xu, D. Y. Tang, S. N. Fu, and L. M. Zhao, "Group velocity locked vector dissipative solitons in a high repetition rate fiber laser," Opt. Express 24, 18718-18726 (2016).
17. G. P. Agrawal, Nonlinear Fiber Optics (Fourth Edition) (2006).